

On the approximation and the optimization of plates

V. Arnautu ^{1,2} H. Langmach ¹ J. Sprekels ¹ D. Tiba ^{1,3}

September, 1997

1991 Mathematics Subject Classification. 49D05.

Keywords. numerical approximation – optimal design – optimal control.

¹Weierstrass Institute for Applied Analysis and Stochastics, Mohrenstrasse 39, D-10117 Berlin, Germany

²Permanent address: University of Iași, Dept. of Mathematics, RO-6600 Iași, Romania

³Permanent address: Institute of Mathematics, Romanian Academy, P.O. Box 1-764, RO-70700 Bucharest, Romania

1 Introduction and preliminaries

This work is devoted to the study of simply supported and of clamped plates. If y denotes the deflection of the plate under the vertical load f and u is the positive thickness of the plate, then we consider the equation

$$(1.1) \quad \Delta(u^3 \Delta y) = f \quad \text{in } \Omega,$$

where $\Omega \subset \mathbb{R}^2$ is a smooth domain. The associated boundary conditions may be

$$(1.2) \quad y = \Delta y = 0 \quad \text{on } \partial\Omega, \quad (\text{simply supported plate})$$

$$(1.3) \quad y = \frac{\partial y}{\partial n} = 0 \quad \text{on } \partial\Omega \quad (\text{clamped plate}).$$

Assuming that $f \in L^2(\Omega)$ (with no sign restrictions) it is well-known that (1.1), (1.2) or (1.1), (1.3) have unique weak solutions in $H^2(\Omega)$. In the recent works of Sprekels and Tiba [8], [9] it is shown that the study of the fourth order partial differential equation (1.1) can be reduced to second order elliptic equations. For the boundary conditions (1.2) such a transformation is very simple and for the boundary conditions (1.3), the result is

Theorem 1.1. (Sprekels and Tiba [9])

The equation (1.1), (1.3) is equivalent with

$$(1.4) \quad \Delta y = g l + h l \quad \text{in } \Omega$$

and (1.3), where $l = u^{-3}$, $h \in L^2(\Omega)$ is harmonic in the sense of distributions in Ω and g satisfies

$$(1.5) \quad \Delta g = f \quad \text{in } \Omega,$$

$$(1.6) \quad g = 0 \quad \text{on } \partial\Omega.$$

In this paper, we use such an approach to develop numerical approximation methods both for Eq. (1.1) and for various optimization problems (optimal control or optimal shape design) that may be associated to it. In Sect. 2, we study the numerical treatment of the clamped plate via second order elliptic systems. Section 3 is devoted to optimization questions. Relevant numerical examples illustrate the application of the proposed methods. In particular, we perform a numerical study of the Hadamard [4] conjecture on the maximum principle for (1.1), (1.3) and its counter-examples.

All the experiments have been made in plane domains given by ellipses with the Ox_1 -semiaxis equal to 1 and the Ox_2 -semiaxis ranging from 0.2 to 1.0 (disc). The discretization of the domains has been obtained by a computer mesh generator which uses a polygonal approximation of the ellipses, the finite elements being triangles.

As shown in Theorem 1.1 and in the subsequent sections, an important ingredient in our numerical schemes has been a FEM solver for the Laplace equation in general plane domains. The corresponding linear algebraic system is obtained starting from the standard variational formulation and using piecewise linear and continuous splines.

Since all the problems that we consider are rewritten as distributed control problems, we use as well optimization procedures of steepest descent type. The standard gradient method is applied in Sect. 2, where unconstrained optimization problems appear. In Sect. 3, we also consider constraints on the control which are handled via a projected gradient method, known as Uzawa's algorithm, Gruver and Sachs [3]. The state constraints are included into the cost functional by a direct penalization in $L^2(\Omega)$.

The linear search in the descent method is based on a robust algorithm due to Legras [6] (see Sect. 3).

2 The clamped plate

The decomposition provided by Theorem 1.1 can be interpreted as an optimality system for distributed control problems governed by second order elliptic equations.

We consider the problem:

$$(2.1) \quad \text{Min} \left\{ \frac{1}{2\varepsilon} \int_{\partial\Omega} \left(\frac{\partial y}{\partial n} \right)^2 + \frac{1}{2} \int_{\Omega} l h^2 \right\}$$

subject to

$$(2.2) \quad \Delta y = h l + l g \quad \text{in } \Omega,$$

$$(2.3) \quad y = 0 \quad \text{on } \partial\Omega.$$

Here $\varepsilon > 0$ is "small" and $l = u^{-3} \in L^\infty(\Omega)$ satisfies

$$(2.4) \quad M^{-3} \leq l(x) \leq m^{-3} \quad \text{a.e. } \Omega$$

(since we take the thickness $u(x)$ in the interval $[m, M], m > 0$).

The equation (2.2), (2.3) has a unique solution $y \in H^2(\Omega) \cap H_0^1(\Omega)$ for any distributed control $h \in L^2(\Omega)$. Moreover, by (2.4), we see that the problem (2.1)–(2.3) is coercive and we get the existence of a unique optimal pair $[y_\varepsilon, h_\varepsilon]$ for any $\varepsilon > 0$.

Theorem 2.1 *There is a unique $p_\varepsilon \in H^1(\Omega)$ solution of the adjoint system*

$$(2.5) \quad \Delta p_\varepsilon = 0 \quad \text{in } \Omega,$$

$$(2.6) \quad p_\varepsilon = \frac{1}{\varepsilon} \frac{\partial y_\varepsilon}{\partial n} \quad \text{on } \partial\Omega,$$

and satisfying the "Pontryagin maximum principle"

$$(2.7) \quad p_\varepsilon + h_\varepsilon = 0 \quad \text{in } \Omega.$$

Proof. Take variations $h_\varepsilon + \lambda K$, $y_\varepsilon + \lambda y_K$, $\lambda \in \mathbb{R}$ with

$$(2.8) \quad \Delta y_K = l K \quad \text{in } \Omega,$$

$$(2.9) \quad y_K = 0 \quad \text{on } \partial\Omega.$$

We obtain

$$\frac{1}{2\varepsilon} \int_{\partial\Omega} \left(\frac{\partial y_\varepsilon}{\partial n} \right)^2 + \frac{1}{2} \int_{\Omega} l h_\varepsilon^2 \leq \frac{1}{2\varepsilon} \int_{\partial\Omega} \left(\frac{\partial y_\varepsilon}{\partial n} + \lambda \frac{\partial y_K}{\partial n} \right)^2 + \frac{1}{2} \int_{\Omega} l (h_\varepsilon + \lambda K)^2$$

for any $\lambda \in \mathbb{R}$ and any $K \in L^2(\Omega)$.

Passing everything to the right-hand side, dividing by λ and letting $\lambda \rightarrow 0^+$, $\lambda \rightarrow 0^-$, we obtain

$$(2.10) \quad \frac{1}{\varepsilon} \int_{\partial\Omega} \frac{\partial y_\varepsilon}{\partial n} \frac{\partial y_K}{\partial n} + \int_{\Omega} l h_\varepsilon K = 0, \quad \forall K \in L^2(\Omega).$$

Multiply (2.5), (2.6) by y_K and integrate by parts to obtain

$$(2.11) \quad 0 = - \int_{\Omega} \Delta p_\varepsilon y_K = \frac{1}{\varepsilon} \int_{\partial\Omega} \frac{\partial y_K}{\partial n} \frac{\partial y_\varepsilon}{\partial n} - \int_{\Omega} p_\varepsilon l K$$

due to (2.8), (2.9).

Then, (2.10), (2.11) yield

$$\int_{\Omega} l h_\varepsilon K + \int_{\Omega} l p_\varepsilon K = 0, \quad \forall K \in L^2(\Omega)$$

that is (2.7) is valid as well.

Remark. We can eliminate p_ε via (2.7) and we obtain the system:

$$(2.12) \quad \Delta y_\varepsilon = h_\varepsilon l + l g \quad \text{in } \Omega,$$

$$(2.13) \quad \Delta h_\varepsilon = 0 \quad \text{in } \Omega,$$

$$(2.14) \quad y_\varepsilon = 0 \quad \text{on } \partial\Omega,$$

$$(2.15) \quad h_\varepsilon = -\frac{1}{\varepsilon} \frac{\partial y_\varepsilon}{\partial n} \quad \text{on } \partial\Omega.$$

We notice that the optimal control $h_\varepsilon \in H^1(\Omega)$ has a better regularity than initially asked and that it is harmonic in Ω .

Theorem 2.2 For $\varepsilon \rightarrow 0$, $\{h_\varepsilon\}$ is bounded in $L^2(\Omega)$ and $\{y_\varepsilon\}$ is bounded in $H^2(\Omega) \cap H_0^1(\Omega)$. Moreover, $\frac{\partial y_\varepsilon}{\partial n} \rightarrow 0$ strongly in $L^2(\partial\Omega)$ and the weak limits $[\tilde{y}, \tilde{h}]$ of $[y_\varepsilon, h_\varepsilon]$ satisfy (1.4), (1.3).

Proof. Take any $\hat{y} \in H_0^2(\Omega)$ and compute $\hat{h} \in L^2(\Omega)$ by the relation

$$\Delta \hat{y} = l \hat{h} + l g \quad \text{in } \Omega,$$

which is possible due to (2.4). The pair $[\hat{y}, \hat{h}]$ is admissible for the problem (2.1)–(2.3) and we have

$$\frac{1}{2\varepsilon} \int_{\partial\Omega} \left(\frac{\partial y_\varepsilon}{\partial n} \right)^2 + \frac{1}{2} \int_{\Omega} l h_\varepsilon^2 \leq \frac{1}{2} \int_{\Omega} l \hat{h}^2, \quad \forall \varepsilon > 0.$$

This shows that $\{h_\varepsilon\}$ is bounded in $L^2(\Omega)$ and $\frac{\partial y_\varepsilon}{\partial n} \rightarrow 0$ strongly in $L^2(\partial\Omega)$. The boundedness of $\{y_\varepsilon\}$ in $H^2(\Omega) \cap H_0^1(\Omega)$ follows by (2.2), (2.3). The passage to the limit in (2.12)–(2.14) to obtain (1.4), (1.3) is obvious.

Remark. By Theorem 2.2 we see that the optimal control problem (2.1)–(2.3) (or equivalently the system (2.12)–(2.14) gives a good approximation of (1.1), (1.3). No boundary conditions are valid for the harmonic mapping h and we do not pass to the limit in (2.15).

Numerical experiments

We have constructed numerical counter-examples to the maximum principle conjecture for the biharmonic operator due to Hadamard [5]. In a recent paper, Tegmark and Shapiro [10] provided an elementary counter-example in the ellipse with semi-axes 1.0 and 0.2 and it is generally accepted in the literature that the Hadamard conjecture is not valid in eccentric ellipses, Duffin [1], Garabedian [2].

Our experiments produced such counter-examples in ellipses with the Ox_1 -semi-axis always equal to 1.0 and the Ox_2 -semi-axis taking different values: 1.0; 0.9; 0.8; 0.7; 0.2. In the case of the disc, it is known that the maximum principle is valid, Michell [7] and our counter-examples concern the case of a nonconstant coefficient in the biharmonic-type operator.

In Table 2.1, we give information on the FEM mesh for the different domains that we consider:

Table 2.1

| | Ox_2 -semiaxis | Nodes | Triangles | Boundary edges |
|---|------------------|-------|-----------|----------------|
| 1 | 1.0 | 4023 | 6863 | 1181 |
| 2 | 0.9 | 3916 | 6698 | 1132 |
| 3 | 0.8 | 3598 | 6106 | 1088 |
| 4 | 0.7 | 3344 | 5642 | 1044 |
| 5 | 0.2 | 1905 | 3215 | 593 |

The numerical solution of (2.1)–(2.3) is very fast and, for $\varepsilon = 10^{-4}$ or 10^{-5} , the computed normal derivative is very accurate in the $L^2(\partial\Omega)$ sense. We have fixed $l(x_1, x_2) = 1$ in Ω , except the case of the disc when

$$(2.16) \quad l(x_1, x_2) = \begin{cases} 1 & \text{if } x_1 \geq 0, x_2 \geq 0, \\ 0.5 & \text{if } x_1 < 0, x_2 < 0, \\ 0.4 & \text{if } x_1 \geq 0, x_2 < 0, \\ 0.3 & \text{if } x_1 < 0, x_2 \geq 0. \end{cases}$$

We recall that under our transformation the thickness of the plate is given by

$$u(x_1, x_2) = l(x_1, x_2)^{-\frac{1}{3}}.$$

The initial choice for the control h was

$$h(x_1, x_2) \equiv 1 \quad \text{in } \Omega.$$

The function $g \in H^2(\Omega) \cap H_0^1(\Omega)$ is the solution to the Laplace equation associated to the load $f \in L^2(\Omega)$. To obtain the counter-examples to the maximum principle, we have tested f in the form of an approximation of a Dirac impulse concentrated in a node close to the extreme points of the semiaxes. The magnitude of f was -10^8 or -10^9 and the points of application were, for instance: $(0.0, 0.895833)$ and $(0.995833, 0.0)$ in the ellipse 2, $(0.995833, 0.0)$ and $(-0.9625, -0.179167)$ in the ellipses 3, respectively 4, $(0.966667, 0.0)$ in the disc 1 (the numbering corresponds to the lines in Table 2.1).

In all the experiments (including the disc with the thickness given via (2.16)), although the force f is negative, the solution takes both positive and negative values. Moreover, the positive maximum was bigger (in absolute value) than the corresponding negative minimum, for each computed solution.

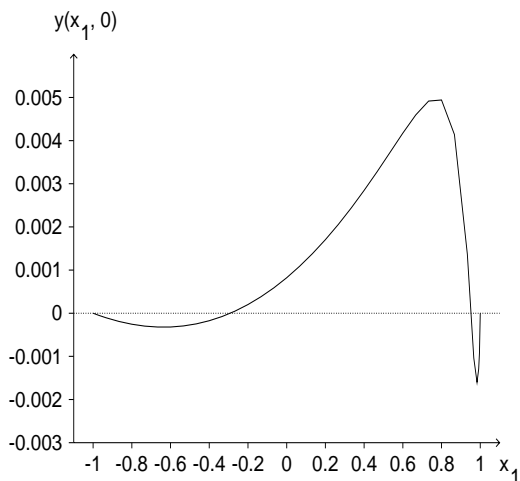


Figure 2.2 a)

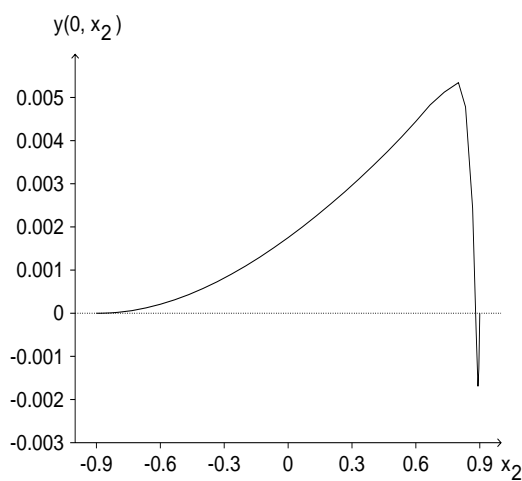


Figure 2.2 b)

Figure 2.2 a) and b) shows the results for the two experiments in the ellipse 2 via sections along the axes of the graph of the solution y .

For the disc of thickness 1.0 (i.e. $l(x_1, x_2) \equiv 1$ in Ω), we have checked various points of application for the Dirac-type load f , but in each case the theoretical result of Michell [7] was observed, that is the value of the solution remained negative.

The algorithm which we have used was a simplified variant of Algorithm 3.1, since no constraints are present and the cost is quadratic.

3 Optimization

We consider first an optimal shape design problem for the simply supported plate:

$$(3.1) \quad \text{Min} \int_{\Omega} u(x) dx$$

subject to (1.1), (1.2). Related problems are

$$(3.2) \quad \text{Min} \int_{\Omega} [-u^{-3}(x)] dx$$

or identification type problems

$$(3.3) \quad \text{Min } \frac{1}{2} \int_{\Omega} [y(x) - y_d(x)]^2 dx$$

with the same state system (1.1), (1.2).

Natural control and state constraints are added:

$$(3.4) \quad y(x) \geq -\tau \quad \text{a.e. in } \Omega,$$

$$(3.5) \quad m \leq u(x) \leq M \quad \text{a.e. in } \Omega.$$

In the paper of Sprekels and Tiba [9] it is shown that the optimization problems (3.1)–(3.3) are respectively equivalent with:

$$(3.6) \quad \text{Min } \int_{\Omega} l^{-\frac{1}{3}}(x) dx,$$

$$(3.7) \quad \text{Min } \int_{\Omega} (-l(x)) dx,$$

$$(3.8) \quad \text{Min } \int_{\Omega} [y(x) - y_d(x)]^2 dx$$

subject to

$$(3.9) \quad \Delta y = g l \quad \text{in } \Omega,$$

$$(3.10) \quad y = 0 \quad \text{on } \partial\Omega,$$

$$(3.11) \quad M^{-3} \leq l(x) \leq m^{-3} \quad \text{a.e. in } \Omega$$

and (3.4).

Let us notice that the distributed control problems (3.6)–(3.10) are similar to those used in the previous section. The main difference is the presence of the control and state constraints (3.11), (3.4).

For the state constraint (3.4), in all the problems where it appears, we shall use a penalization approximation by adding to the original cost the term

$$(3.12) \quad \frac{1}{2\varepsilon} \int_{\Omega} [y(x) + \tau]_-^2.$$

For the control constraints (3.11) a projected gradient method is used.

Denote the cost functional of the penalized control problem by

$$(3.13) \quad \Phi(l, y) = J(l) + \varphi(y),$$

where $J(l)$ is the functional given in formula (3.6) or (3.7) and $\varphi(y)$ is given by (3.12). In the case of the identification problem we take

$$(3.14) \quad \Phi(l, y) = K(y) = \varphi(y)$$

with $K(y)$ given in (3.8).

We define the adjoint system by:

$$(3.15) \quad \begin{cases} \Delta p &= -\frac{1}{\varepsilon}(y + \tau)_- & \text{in } \Omega, \\ p &= 0 & \text{on } \partial\Omega, \end{cases}$$

for (3.13) and by

$$\begin{cases} \Delta p &= y - y_d - \frac{1}{\varepsilon}(y + \tau)_- & \text{in } \Omega \\ p &= 0 & \text{on } \partial\Omega, \end{cases}$$

for (3.14).

Accordingly, the gradient of $l \rightarrow \Phi(l, y)$ is given by $\nabla\Phi(l) = \nabla J(l) + p g$ for (3.13) and by $\nabla\Phi(l) = p g$ for (3.14).

We give now the algorithm corresponding to (3.13).

Algorithm 3.1

S0 Compute g as the solution of

$$\begin{cases} \Delta g &= f & \text{in } \Omega, \\ g &= 0 & \text{on } \partial\Omega. \end{cases}$$

$L_{\text{old}} := l^{(0)}$

S1 Compute y as the solution of the state system

$$\begin{cases} \Delta y &= g L_{\text{old}} & \text{in } \Omega, \\ y &= 0 & \text{on } \partial\Omega. \end{cases}$$

S2 Compute p as the solution of the adjoint system (3.15).

S3 $\nabla\Phi := \nabla J(L_{\text{old}}) + g p$.

S4 Compute ρ , the step length of the projected gradient method.

S5 $L_{\text{new}} := \text{Proj}(L_{\text{old}} - \rho \nabla\Phi)$.

S6 the stopping criterion:

IF $\|L_{\text{new}} - L_{\text{old}}\|_{L^2(\Omega)} < \delta$
 THEN STOP
 ELSE $L_{\text{old}} := L_{\text{new}}$; GO TO **S1**

Here Proj is the projection (pointwise) operator corresponding to the control constraints (3.11) and $\delta > 0$ is a prescribed precision. Let us point out that ρ in **S4** is obtained by the algorithm due to Legras [6].

Consider $\phi(\rho) = \Phi(L_{\text{old}} - \rho \nabla\Phi)$ and $\bar{\rho}$ a starting value for the search procedure (which is obtained from the previous iteration). We consider the following values of ϕ : $\phi_0 = \Phi(L_{\text{old}})$, $\phi_1 = \Phi(L_{\text{old}} - \bar{\rho} \nabla\Phi)$, $\phi_2 = \Phi(L_{\text{old}} - 2\bar{\rho} \nabla\Phi)$. Let us also mention that first $\bar{\rho}$ is divided by 4 until $\phi_1 < \phi_0$. The pairs $(0, \phi_0)$, $(\bar{\rho}, \phi_1)$ and $(2\bar{\rho}, \phi_2)$ are interpolated by a second degree polynomial q which is given by

$$q(\rho) = \frac{1}{2\bar{\rho}^2}(\phi_0 - 2\phi_1 + \phi_2)\rho^2 - \frac{1}{2\bar{\rho}}(3\phi_0 - 4\phi_1 + \phi_2)\rho + \phi_0.$$

If $\phi_0 - 2\phi_1 + \phi_2 > 0$, then

$$\rho^* = \frac{1}{2} \bar{\rho} \frac{3\phi_0 - 4\phi_1 + \phi_2}{\phi_0 - 2\phi_1 + \phi_2}$$

is the minimum point of q and ρ is chosen such that

$$\phi(\rho) = \min \{ \phi(\bar{\rho}), \phi(2\bar{\rho}), \phi(\rho^*) \}.$$

If $\phi_0 - 2\phi_1 + \phi_2 \leq 0$ then ρ^* is no longer a minimum point for q , which means that the interpolation process is not fine enough. In this case ρ is chosen such that

$$\phi(\rho) = \min \{ \phi(\bar{\rho}), \phi(2\bar{\rho}) \}.$$

We have performed numerical experiments with the cost functionals (3.6) and (3.8). The domain Ω was the ellipse 5 (see Table 2.1). The initial thickness was $l_0 = 0.3$ satisfying the ‘‘control constraints’’ $0.1 \leq l(x_1, x_2) \leq 19.9$ and $u_0 = l_0^{-1/3}$. The fixed load was assumed to take two different values in two different halves of the ellipse:

$$\begin{aligned} f(x_1, x_2) &= -1000 & x_1 \geq 0, \\ f(x_1, x_2) &= -2000 & x_1 < 0, \end{aligned}$$

(and similarly with respect to x_2). In all the tests, we have fixed $\tau = 0.1$ in (3.4). Significant decrease in the thickness (minimum 20 %) was noticed in all the experiments. The obtained state satisfied the state constraints (with minor variations) and the active points were on the horizontal axis.

We have also imposed $f(x_1, x_2) = -100$ in Ω and, then, a much more important decrease in the thickness was noticed.

Another experiment considered

$$\begin{aligned} f(x_1, x_2) &= 200 & x_1 \geq 0, \\ f(x_1, x_2) &= -2500 & x_1 < 0, \end{aligned}$$

since our approach does not need the maximum principle (although it is valid for simply supported plates). Then, the active nodes are on the negative Ox_1 -semiaxis, corresponding to the negative load.

The Figure 3.1 a) and b) and the Figure 3.2 a) and b) represent the optimal l (denoted by L) in this last case, respectively in the case $f(x_1, x_2) \equiv -1000$ in Ω , together with its section along the axis $x_2 = 0$. Recall that the thickness $u(x_1, x_2)$ is given by $u(x_1, x_2) = l(x_1, x_2)^{-\frac{1}{3}}$ and notice the bang-bang type properties of l put into evidence in Figure 3.1 b). Figure 3.1 a) takes into account the influence of the non-symmetric load. Moreover, both Figure 3.1 a) and Figure 3.2 a) show that the optimal thickness on the boundary is given by the lower possible limit.

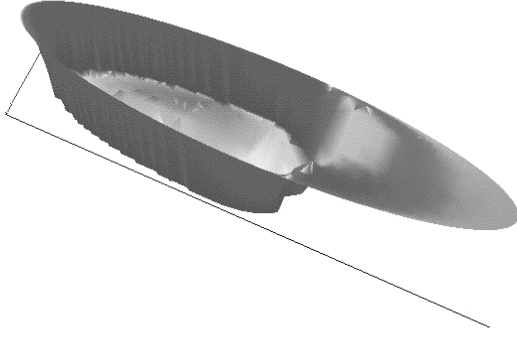


Figure 3.1 a)

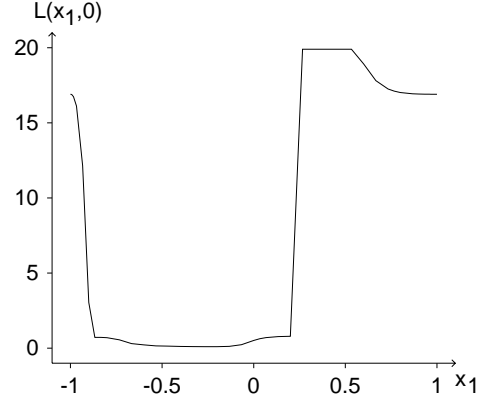


Figure 3.1 b)

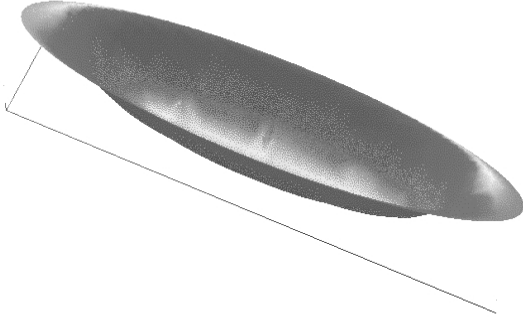


Figure 3.2 a)

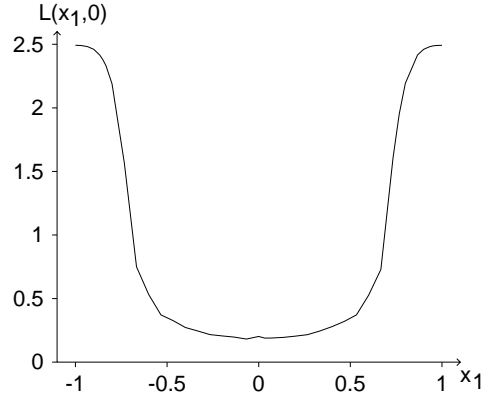


Figure 3.2 b)

As a general remark, the convergence of Algorithm 3.1 was slow since the functional (3.6) has, naturally, a very slowly decreasing slope. This reflects the difficulty of the original shape optimization problem, which for f with changing sign, is not even convex (see Sprekels and Tiba [9]). However, the cost (3.6) is strictly convex.

In the case of the functional (3.8), this property is lost and the identification-type problem has nonunique solutions, in general. We have chosen $y_d(x_1, x_2) = (x_1^2 + 25x_2^2 - 1)^3$ and

$$f(x_1, x_2) = 48960x_1^2 + 5.716.800x_2^2 - 46272.$$

Then, y_d is the solution, corresponding to f and to $u(x_1, x_2) = 1$ in Ω , of (1.1), (1.2). That is $l(x_1, x_2) = u^{-3}(x_1, x_2) = 1$ in Ω is the solution to (3.8)–(3.11).

We have tested Algorithm 3.1 with various initial guesses $l_0(x_1, x_2) : 5; 1.2; 1.05; 1.005$ (constant in Ω). There are no state constraints and the control constraints

are $0.1 \leq l(x_1, x_2) \leq 9.9$. The value of the cost is decreased practically to the optimal value (which equals 0), but another solution for l is found, in general. However, in the last test with $l_0(x_1, x_2) = 1.005$ in Ω , convergence of the solution to the “true” solution $l(x_1, x_2) = 1$ in Ω was noticed.

Another type of distributed optimal control problem that we have tested is the maximal admissible load of a clamped plate. This can be formulated as follows

$$(3.16) \quad \text{Min} \int_{\Omega} f(x) dx,$$

$$(3.17) \quad \Delta(u^3 \Delta y) = f \quad \text{in } \Omega,$$

$$(3.18) \quad y = \frac{\partial y}{\partial n} = 0 \quad \text{on } \partial\Omega,$$

$$(3.19) \quad -K \leq f(x) \leq 0 \quad \text{a.e. in } \Omega$$

and (3.4).

Here $u \in L^\infty(\Omega)_+$ is a given thickness. The state constraint (3.4) is directly penalized in the cost by (3.12).

The problem (3.16)–(3.19), (3.4) has an intrinsic interest, but it is important as well for the subsequent solution of the optimal shape design problems (u is the minimization parameter) (3.1)–(3.3) associated to the clamped plate (3.17), (3.18) via the dual approach proposed by Sprekels and Tiba [8], [9]. The algorithm for the solution of (3.17), (3.18) is the one indicated in Sect. 2. This is as well applied to the solution of the adjoint system:

$$(3.20) \quad \Delta(u^3 \Delta p) = -\frac{1}{\varepsilon}(y + \tau)_- \quad \text{in } \Omega,$$

$$(3.21) \quad p = 0, \quad \frac{\partial p}{\partial n} = 0 \quad \text{on } \partial\Omega.$$

Here, the right-hand side in (3.20) is due to the penalization in the cost functional of (3.4) via (3.12). The gradient of the penalized cost is obtained as follows:

$$(3.22) \quad \nabla J(f) = 1 + p \quad \text{in } \Omega.$$

Then, relations (3.20)–(3.22) may be used in Algorithm 3.1 for the numerical solution of the problem (3.16)–(3.19).

In the experiments, we fix again Ω given by ellipse 5. The lower bound on the control in (3.19) was $K = -10.000$. The penalization parameter for the state constraints was $\varepsilon = 10^{-7}$ and $\tau = 0.1$. The penalization parameter in (2.1) was $\varepsilon = 10^{-5}$ (used for the solution of (3.17), (3.18) or of (3.20), (3.21)).

The initial guess for the load was $f_0(x_1, x_2) = -10$ in Ω with the initial cost equal to $-6.28 \dots$. One test assumed $u(x_1, x_2) = 1$ in Ω . After 37 iterations, the cost was decreased to $-4101.79 \dots$ and the state constraints are fulfilled with minor violations.

Another experiment took

$$\begin{aligned}u(x_1, x_2) &= 1 && \text{if } x_1 \geq 0, x_2 \geq 0, \\u(x_1, x_2) &= 1.25 && \text{if } x_1 < 0, x_2 < 0, \\u(x_1, x_2) &= 1.4 && \text{if } x_1 \geq 0, x_2 < 0, \\u(x_1, x_2) &= 1.5 && \text{if } x_1 < 0, x_2 \geq 0.\end{aligned}$$

After 9 iterations the cost was decreased from $-6.28\dots$ to -5730.36 and the solution satisfied the constraints with minor violations.

The convergence was very quick, in contrast to the identification or optimal shape design problems.

References

- [1] Duffin, R. J.: On a question of Hadamard concerning super-biharmonic functions. *J. Math. and Phys.* **27** (1949) 253–258
- [2] Garabedian, P. R.: A partial differential equation arising in conformal mapping. *Pacific J. Math.* **1** (1951) 485–524
- [3] Gruver, W. A., Sachs, E.: *Algorithmic methods in optimal control*. Pitman Research Notes in Mathematics **47**, Pitman, London (1981)
- [4] Hadamard, J.: Mémoire sur le problème d’analyse relatif à l’équilibre des plaques élastiques encastrées. *Mémoires présentés à l’Académie des Sciences* **33** (1908) 516–629
- [5] Hadamard, J.: *Oeuvres*. Vols. 1–4, Editions du Centre National de la Recherche Scientifique, Paris (1968)
- [6] Legras, J.: *Algorithmes et programmes d’optimisation non linéaire avec contraintes*. Masson, Paris (1980)
- [7] Michell, J. H.: The flexure of a circular plate. *Proc. London Math. Soc.* **34** (1901) 223–228
- [8] Sprekels, J., Tiba, D.: A duality-type method for the design of beams. to appear in *Adv. Math. Sci. Appl.*, Gakkotōsho, Tokyo
- [9] Sprekels, J., Tiba, D.: A duality approach in the optimization of beams and plates. Preprint 335, WIAS, Berlin (1997)
- [10] Tegmark, M., Shapiro, H. S.: An elementary proof that the biharmonic Green function of an eccentric ellipse changes sign. *SIAM Review*, vol. 36, no. 1 (1994) 99–101